

# Effects of In-Plane Shear Loads on Transverse Shear Deformations in Composite Panels

Jingbo Wang\*

*ExxonMobil Research and Engineering Company, Annandale, New Jersey 08801*

and

James L. Glancey<sup>†</sup> and Jack R. Vinson<sup>‡</sup>

*University of Delaware, Newark, Delaware 19716*

DOI: 10.2514/1.27913

An analytical and experimental investigation is performed to clarify the transverse shear deformations that occur in laminated and sandwich composite plates subjected to in-plane shear loads. This is part of a larger study investigating the feasibility of an in-plane shear test as a practical procedure to determine the in-plane shear modulus and/or strength of various material systems as well as the faces and cores of sandwich plates. The theorem of minimum potential energy has been used to determine the deflections and strains in the plate, including the transverse shear deformation effects. Polynomial functions that satisfy all the boundary conditions of the material system are used as trial functions. Comparison of these solutions to those first proposed by Nadai in 1925 revealed that additional terms are added to the original analysis (which used classical plate theory) to incorporate these effects. The methods developed clearly show the effects of the transverse shear deformation and are valid for any sandwich, laminate, or monocoque plate of any aspect ratio. Subsequent finite element and experimental analysis were conducted to verify the analytical study. Both the numerical and experimental results confirm that the analytical results are very good approximations for describing the linear deformation of the panels subject to in-plane shear loads.

## I. Introduction

WITH the rapidly increasing use of composite materials over the world, fast, accurate, and inexpensive testing procedures for determining mechanical properties are needed. This goal is crucial for the design and optimization of advanced, complex composite structures. The in-plane shear test described herein appears to be a promising method to determine the in-plane shear modulus and strength of the composite materials used in laminated and sandwich panels. Figure 1 shows the loading condition of a rectangular plate for determining the in-plane shear strength and stiffness. In this configuration, loads of equal magnitude and direction are applied to two diagonal corners of the plate, and reacted at the two opposite corners.

The concept of an in-plane shear test for isotropic plates was first suggested by Nadai [1] in 1925. He solved the problem in an analytical way by finding a solution to the governing partial differential equations, which are derived from classical continuum mechanics. Recently, Vinson [2] derived a very simple expression to determine the in-plane shear strength of the composite materials in laminated and sandwich structures using the minimum potential energy method. As a special case, Vinson provided the equations for the in-plane shear strength of the face material, the core material, and the adhesive bond between the faces and the core for sandwich plate structures. Motivated by this analysis, Ebrahimpour et al. [3] conducted an experimental and numerical study to characterize the behavior of foam core sandwich composite plates subjected to in-plane shear loads.

This study described herein presents a solution including transverse shear deformation effects for this problem. The investigation of

the transverse shear deformation effects is essential to better understand the behavior of the composite structures under the in-plane shear loading, especially for those plates having low transverse shear moduli  $G_{13}$  and  $G_{23}$ . This analysis follows the same methodology used by Vinson [2] and Wang et al. [4]. Numerical and experimental studies are used to verify the analytical conclusions. The primary motivation is to investigate the suitability of the in-plane shear test for improved manufacturing quality control of laminated and sandwich composite plates.

## II. Analysis

Linear thin plate theories are assumed for the plates considered in this study; specifically, the thickness of the plate is much smaller than the other dimensions of the plate, and the plate experiences small lateral deflections. In the analysis that follows, all of the plates including isotropic, laminated, and sandwich structures are rectangular with no restriction of the aspect ratio. All surfaces are load free, and all composite plates are midplane symmetric and are specially orthotropic, that is, no 16 and 26 terms in the constitutive equations.

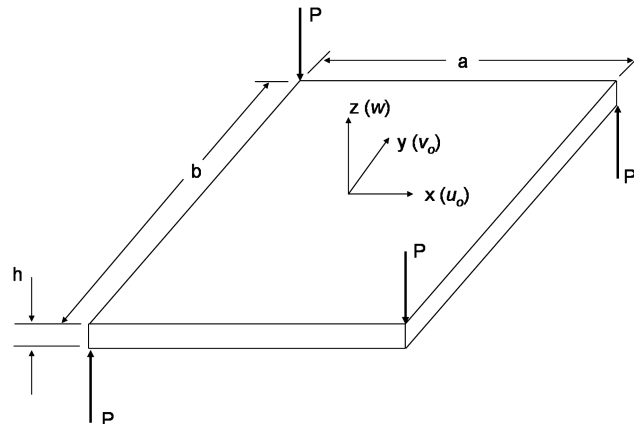


Fig. 1 Plate configuration and loading for the in-plane shear test.

Received 19 September 2006; revision received 8 May 2009; accepted for publication 12 May 2009. Copyright © 2009 by the American Institute of Aeronautics and Astronautics, Inc. All rights reserved. Copies of this paper may be made for personal or internal use, on condition that the copier pay the \$10.00 per-copy fee to the Copyright Clearance Center, Inc., 222 Rosewood Drive, Danvers, MA 01923; include the code 0021-8669/09 and \$10.00 in correspondence with the CCC.

\*Research Engineer, Downstream Petroleum Sciences Lab, Corporate Strategic Research.

<sup>†</sup>Associate Professor, Department of Mechanical Engineering.

<sup>‡</sup>H. Fletcher Brown Professor, Department of Mechanical Engineering.

Considering the linear thin plate assumptions and the plate structure attributes described above, and that first order shear deformation theory describes the plate kinematics, the potential energy expression including transverse shear deformation effects for plates subjected to the loads shown in Fig. 1 can be written in the following form [3]:

$$\begin{aligned}
 V = & \int_{-\frac{a}{2}}^{\frac{a}{2}} \int_{-\frac{b}{2}}^{\frac{b}{2}} \left\{ \frac{A_{11}}{2} \left( \frac{\partial u_0}{\partial x} \right)^2 + \frac{D_{11}}{2} \left( \frac{\partial \bar{\alpha}}{\partial x} \right)^2 + A_{12} \frac{\partial u_0}{\partial x} \frac{\partial v_0}{\partial y} \right. \\
 & + D_{12} \frac{\partial \bar{\beta}}{\partial y} \frac{\partial \bar{\alpha}}{\partial x} + \frac{A_{22}}{2} \left( \frac{\partial v_0}{\partial y} \right)^2 + \frac{D_{22}}{2} \left( \frac{\partial \bar{\beta}}{\partial y} \right)^2 + A_{66} \left[ \frac{1}{2} \left( \frac{\partial u_0}{\partial y} \right)^2 \right. \\
 & + \frac{\partial u_0}{\partial y} \frac{\partial v_0}{\partial x} + \frac{1}{2} \left( \frac{\partial v_0}{\partial x} \right)^2 \left. \right] + D_{66} \left[ \frac{1}{2} \left( \frac{\partial \bar{\alpha}}{\partial y} \right)^2 + \frac{\partial \bar{\alpha}}{\partial x} \frac{\partial \bar{\beta}}{\partial y} \right. \\
 & + \frac{1}{2} \left( \frac{\partial \bar{\beta}}{\partial x} \right)^2 \left. \right] + A_{45} \left[ \bar{\alpha} \bar{\beta} + \bar{\alpha} \frac{\partial w}{\partial y} + \bar{\beta} \frac{\partial w}{\partial x} + \frac{\partial w}{\partial x} \frac{\partial w}{\partial y} \right] \\
 & + A_{55} \left[ \frac{\bar{\alpha}^2}{2} + \bar{\alpha} \frac{\partial w}{\partial x} + \frac{1}{2} \left( \frac{\partial w}{\partial x} \right)^2 \right] + A_{44} \left[ \frac{\bar{\beta}^2}{2} + \bar{\beta} \frac{\partial w}{\partial y} \right. \\
 & + \left. \frac{1}{2} \left( \frac{\partial w}{\partial y} \right)^2 \right] \left. \right\} dx dy - Pw \left( \frac{a}{2}, \frac{b}{2} \right) - Pw \left( -\frac{a}{2}, -\frac{b}{2} \right) \\
 & + Pw \left( \frac{a}{2}, -\frac{b}{2} \right) + Pw \left( -\frac{a}{2}, \frac{b}{2} \right) \quad (1)
 \end{aligned}$$

In Eq. (1),  $u_0$  and  $v_0$  are the in-plane midsurface displacements in the  $x$  and  $y$  directions, respectively,  $w$  is the lateral displacement, and  $\bar{\alpha}$  and  $\bar{\beta}$  are the rotations in the  $x$  and  $y$  directions, respectively. The quantities  $a$  and  $b$  are the plate dimensions in the  $x$  and  $y$  directions, respectively. The  $A_{ij}$  and  $D_{ij}$  terms are components of the integrated in-plane stiffness and flexural stiffness matrix.  $P$  is the applied load at the corners as shown in Fig. 1.

The most general methodology for using the minimum potential energy theorem is to assume the displacement functions according to an estimated deformed shape that satisfies all boundary conditions. In the following, polynomials are chosen as trial functions to approximate the midplane displacements, rotations, and curvatures. One advantage of choosing polynomials is a result of the geometric symmetry of this problem; many terms of the polynomial expansions can be canceled. In addition, the estimated shape of these plates after deformation is similar to a two-dimensional polynomial surface, and it is also easy to manipulate the polynomials in differential, expanding, and integral operations.

If the Kirchhoff hypothesis used in classical lamination theory is relaxed to permit independent rotations about the  $x$  and  $y$  axes, the linear strain-displacement relations are [5]

$$\varepsilon_x = \frac{\partial u}{\partial x} = \frac{\partial u_0}{\partial x} + z \frac{\partial \bar{\alpha}}{\partial x} \quad (2)$$

$$\varepsilon_y = \frac{\partial v}{\partial y} = \frac{\partial v_0}{\partial y} + z \frac{\partial \bar{\beta}}{\partial y} \quad (3)$$

$$\varepsilon_z = \frac{\partial w}{\partial z} = \frac{\partial w_0}{\partial z} = 0 \quad (4)$$

$$\varepsilon_{xy} = \frac{1}{2} \left( \frac{\partial u}{\partial y} + \frac{\partial v}{\partial x} \right) = \varepsilon_{xy0} + z \kappa_{xy} \quad (5)$$

$$\varepsilon_{xz} = \frac{1}{2} \left( \frac{\partial u}{\partial z} + \frac{\partial w}{\partial x} \right) = \frac{1}{2} \left( \bar{\alpha} + \frac{\partial w}{\partial x} \right) \quad (6)$$

$$\varepsilon_{yz} = \frac{1}{2} \left( \frac{\partial v}{\partial z} + \frac{\partial w}{\partial y} \right) = \frac{1}{2} \left( \bar{\beta} + \frac{\partial w}{\partial y} \right) \quad (7)$$

where the midplane strains can be represented as

$$\varepsilon_{x0} = \frac{\partial u_0}{\partial x}, \quad \varepsilon_{y0} = \frac{\partial v_0}{\partial y}, \quad \varepsilon_{xy0} = \frac{1}{2} \left( \frac{\partial u_0}{\partial y} + \frac{\partial v_0}{\partial x} \right) \quad (8)$$

and the curvatures can be represented as

$$\kappa_x = \frac{\partial \bar{\alpha}}{\partial x}, \quad \kappa_y = \frac{\partial \bar{\beta}}{\partial y}, \quad \kappa_{xy} = \frac{1}{2} \left( \frac{\partial \bar{\alpha}}{\partial y} + \frac{\partial \bar{\beta}}{\partial x} \right) \quad (9)$$

Third-order polynomials are selected to act as the deflection functions, the midplane displacement functions, and the curvature functions. Note that with the inclusion of transverse shear deformation effects, the rotation functions  $\bar{\alpha}$  and  $\bar{\beta}$  are not first derivatives of the lateral displacement, and therefore are expressed as independent polynomial functions. The assumed functions are defined as follows:

$$\begin{aligned}
 w(x, y) = & C_1 + C_2x + C_3y + C_4x^2 + C_5xy + C_6y^2 \\
 & + C_7x^3 + C_8x^2y + C_9xy^2 + C_{10}y^3 \\
 u_0(x, y) = & A_1 + A_2x + A_3y + A_4x^2 + A_5xy + A_6y^2 \\
 & + A_7x^3 + A_8x^2y + A_9xy^2 + A_{10}y^3 \\
 v_0(x, y) = & B_1 + B_2x + B_3y + B_4x^2 + B_5xy + B_6y^2 \\
 & + B_7x^3 + B_8x^2y + B_9xy^2 + B_{10}y^3 \\
 \bar{\alpha}(x, y) = & D_1 + D_2x + D_3y + D_4x^2 + D_5xy + D_6y^2 \\
 & + D_7x^3 + D_8x^2y + D_9xy^2 + D_{10}y^3 \\
 \bar{\beta}(x, y) = & E_1 + E_2x + E_3y + E_4x^2 + E_5xy + E_6y^2 \\
 & + E_7x^3 + E_8x^2y + E_9xy^2 + E_{10}y^3 \quad (10)
 \end{aligned}$$

Upon examination of Fig. 1, it is seen that

$$\begin{aligned}
 w(0, 0) = u_0(0, 0) = v_0(0, 0) = \bar{\alpha}(0, 0) = \bar{\beta}(0, 0) = 0 \\
 \frac{\partial w}{\partial x}(0, 0) = 0, \quad \frac{\partial w}{\partial y}(0, 0) = 0
 \end{aligned}$$

and

$$w(x, y) = w(-x, -y) = -w(-x, y) = -w(x, -y)$$

The corresponding boundary conditions are

$$\begin{aligned}
 N_x = N_{xy} = M_x = M_{xy} = 0 \text{ on } x = \pm \frac{a}{2} \\
 N_y = N_{xy} = M_y = M_{xy} = 0 \text{ on } y = \pm \frac{b}{2}
 \end{aligned}$$

After applying these requirements and boundary conditions, the displacement and curvature functions are reduced to

$$w(x, y) = C_5xy \quad (11)$$

$$u_0(x, y) = A_3y, \quad v_0(x, y) = B_2x, \quad A_3 + B_2 = 0 \quad (12)$$

$$\bar{\alpha}(x, y) = D_3y + D_6y^2 + D_{10}y^3 \quad (13)$$

$$\bar{\beta}(x, y) = E_2x + E_4x^2 + E_7x^3 \quad (14)$$

To get a concise, practical, and usable expression for strain distribution, another assumption that the in-plane shear strain distributes linearly with respect to  $x$  and  $y$  is adopted here to further simplify the curvature functions as

$$\bar{\alpha}(x, y) = D_3y + D_6y^2, \quad \bar{\beta}(x, y) = E_2x + E_4x^2 \quad (15)$$

After substituting these functions into the potential energy function [1] and performing the integration and the variation operations, a set of five algebraic equations are obtained as follows, where the unknowns are the coefficients in the variables  $\delta w$ ,  $\delta \bar{\alpha}$ ,  $\delta \bar{\beta}$ ,  $\delta u_0$ , and  $\delta v_0$ :

$$\begin{aligned} D_{66}(D_3 + E_2) + \frac{1}{12}A_{55}b^2(D_3 + C_5) &= 0 \\ D_{66}(D_3 + E_2) + \frac{1}{12}A_{44}a^2(E_2 + C_5) &= 0 \\ \frac{1}{3}D_{66}D_6 + \frac{1}{144}A_{45}a^2E_4 + \frac{1}{80}A_{55}b^2D_6 &= 0 \\ \frac{1}{3}D_{66}E_4 + \frac{1}{144}A_{45}b^2D_6 + \frac{1}{80}A_{44}a^2E_4 &= 0 \\ \frac{1}{12}A_{55}b^2(D_3 + C_5) + \frac{1}{12}A_{44}a^2(E_2 + C_5) - P &= 0 \end{aligned} \quad (16)$$

Solving these equations for the five unknowns gives

$$\begin{aligned} C_5 &= \frac{P}{4D_{66}} + 3\left(\frac{A_{55}b^2 + A_{44}a^2}{A_{44}A_{55}a^2b^2}\right)P \\ D_3 &= -\frac{P}{4D_{66}} + 3\left(\frac{A_{44}a^2 - A_{55}b^2}{A_{44}A_{55}a^2b^2}\right)P \\ E_2 &= -\frac{P}{4D_{66}} + 3\left(\frac{A_{55}b^2 - A_{44}a^2}{A_{44}A_{55}a^2b^2}\right)P, \quad D_6 = E_4 = 0 \\ w(x, y) &= \frac{P}{4D_{66}}xy + 3\left(\frac{A_{55}b^2 + A_{44}a^2}{A_{55}A_{44}a^2b^2}\right)Pxy \end{aligned} \quad (17)$$

Note that cases where either  $a \gg b$  or  $a \ll b$  could cause one of the two transverse stiffness terms to become predominant. And as expected, the effect of transverse shear deformation on plate deflection decreases as  $a$  and  $b$  increase.

All of the constants are now known, and all normal in-plane strains and stresses are zero. In addition, there are no curvatures in the plate in any direction. The shear strains and stresses can be expressed as

$$[\varepsilon_{xy}]_k = -\frac{P}{4D_{66}}z, \quad [\sigma_{xy}]_k = -\frac{[\bar{Q}_{66}]_k P}{2D_{66}}z \quad (18)$$

$$[\varepsilon_{xz}]_k = \frac{3P}{A_{55}b^2}y, \quad [\sigma_{xz}]_k = \frac{6P[\bar{Q}_{45}]_k}{A_{44}a^2}x + \frac{6P[\bar{Q}_{55}]_k}{A_{55}b^2}y \quad (19)$$

$$[\varepsilon_{yz}]_k = \frac{3P}{A_{44}a^2}x, \quad [\sigma_{yz}]_k = \frac{6P[\bar{Q}_{44}]_k}{A_{44}a^2}x + \frac{6P[\bar{Q}_{45}]_k}{A_{55}b^2}y \quad (20)$$

The in-plane shear strains and stresses are independent of the in-plane coordinates  $x$  and  $y$  due to the canceling of  $D_6$  and  $E_4$ . This result agrees with the Vinson and Sierakowski [6] analysis which used classical plate theory. Therefore, the transverse shear deformation effects do not influence the in-plane shear strains and stresses. An additional term  $3[(A_{55}b^2 + A_{44}a^2)/A_{44}A_{55}a^2b^2]Pxy$  involving the cross-thickness transverse shear moduli ( $A_{44}$  and  $A_{55}$ ) now appears in the lateral displacement function when compared to the expression provided by Vinson [2]. It is reasonable that the transverse shear deformation contributes to the lateral deflection but does not affect the in-plane deformation quantities. It is seen that the transverse shear deformation effects decrease with increasing values of the cross-thickness transverse shear moduli. When  $A_{44}$  and  $A_{55}$  approach infinity, the second term goes to zero and  $w(x, y)$  reverts to the same form as derived by Vinson and Sierakowski [6], using classical plate theory.

To clarify the extent of the transverse shear deformation effects on the deformation of the plate, it is helpful to 1) compare the magnitudes of the transverse shear strains with the magnitude of the in-plane shear strain  $\varepsilon_{xy}$ , and 2) obtain the ratio of the second term in

the lateral deflection function, which reflects the transverse shear deformation effects, to the first term of that function.

If the plate is constructed using isotropic materials, the ratio of the transverse shear deformation term in the lateral deflection function to the first term is  $1.2h^2(b^2 + a^2)/a^2b^2$ . For thin plate structures, the in-plane dimensions are generally much larger than the thickness. If, for example,  $a = b = 10h$ , the ratio is 0.024, and it is obvious that the effects of the transverse shear deformation on the lateral deflection of the isotropic plates are quite insignificant. In the case of composite laminates or sandwich plates, the extent of the transverse shear effects on the lateral displacement depends on the value of  $12D_{66}[(A_{55}b^2 + A_{44}a^2)/A_{44}A_{55}a^2b^2]$ , which is a function of the individual material system.

From Eqs. (19) and (20), it is seen that the magnitudes of the transverse shear strains are dependent on the values of the coordinates  $x$  and  $y$ . To compare the extreme values, ratios of transverse shear strains with  $\varepsilon_{xy}$ ,  $|\varepsilon_{xz}|_{\max}/|\varepsilon_{xy}|$  and  $|\varepsilon_{yz}|_{\max}/|\varepsilon_{xy}|$  are investigated as follows:

1) For the isotropic plates,

$$\frac{|\varepsilon_{xz}|_{\max}}{|\varepsilon_{xy}|} = \frac{6h}{5b}, \quad \frac{|\varepsilon_{yz}|_{\max}}{|\varepsilon_{xy}|} = \frac{6h}{5a}$$

In most cases, the thickness of the plate is much smaller than the length and width of the plate. Therefore, these two ratios can be expected to be low.

2) For laminated or sandwich composite plates,

$$\frac{|\varepsilon_{xz}|_{\max}}{|\varepsilon_{xy}|} = \frac{12D_{66}}{A_{55}bh}$$

and

$$\frac{|\varepsilon_{yz}|_{\max}}{|\varepsilon_{xy}|} = \frac{12D_{66}}{A_{44}ah}$$

which both depend on the specific values of material properties of the structures.

### III. Numerical Simulations

A finite element model of a laminated composite plate was first created in ANSYS [7] to perform the numerical study. Material properties are taken from Kant and Swaminathan [5]. For each layer of the plate, it is given that

$$E_{11} = 172.37 \text{ GPa}, \quad E_{22} = E_{33} = 6.89 \text{ GPa}$$

$$\nu_{12} = \nu_{13} = \nu_{23} = 0.25, \quad G_{12} = G_{13} = 3.45 \text{ GPa}$$

$$G_{23} = 1.38 \text{ GPa}$$

In modeling the plate, eight equal-thickness layers are stacked orthogonally so that the two face layers are oriented in the same direction as the global coordinate and the structure is symmetric about the midplane. The plate dimensions are  $304.8 \times 304.8 \times 10.16$  mm.

Using the material properties listed above, the cross-thickness stiffness quantities are

$$D_{66} = 301.33 \text{ N} \cdot \text{m}, \quad A_{44} = 2.21 \times 10^7 \text{ N/m}$$

$$A_{55} = 1.87 \times 10^7 \text{ N/m}$$

For this example, the following ratios are also computed:

$$\frac{|\varepsilon_{xz}|_{\max}}{|\varepsilon_{xy}|} = 0.06$$

and

$$\frac{|\varepsilon_{yz}|_{\max}}{|\varepsilon_{xy}|} = 0.05$$

Also, one is able to calculate the ratio of the second term in  $w$ , which represents the effects of the transverse shear deformation, to the first term. This ratio is less than 0.004. It is clear that the magnitudes of the transverse shear strains are much smaller than the magnitude of the in-plane shear strain, and the transverse shear deformation effects do not make significant contributions to the deflection of the plate.

In the finite element models, two different elements were used for the 3-D elastic modeling of the solid structures. The first element was defined by eight nodes having 3 degrees of freedom at each node: translations in the nodal  $x$ ,  $y$ , and  $z$  directions (SOLID46 in ANSYS). This element included up to 250 unique layers designed to model laminated thick shells and solids. The second element, a 20 node element with similar degrees of freedom and layering characteristics (SOLID191 in ANSYS), was used to create higher resolution models of the plates. For both the 8 and 20 node element models, elements were square and had the identical size ( $10.16 \times 10.16 \times 10.16$  mm).

For all simulations, the boundary conditions of the plate are constrained to zero displacements in all directions at the centroids of the top and bottom faces. Loads were applied in each corner of the plate the same manner illustrated in Fig. 1.

Comparison of the numerical solutions revealed no significant differences between the 8 and 20 node element models. Numerical results indicate that the in-plane shear strain  $\varepsilon_{xy}$  is the dominant strain. All the other normal and shear strains are much smaller than the magnitude of  $\varepsilon_{xy}$ . This result agrees with the analytical conclusion stated previously that the transverse shear strains can be ignored. It can also be concluded that the in-plane shear strain is the primary factor in determining the failure of the laminated plate structures subjected to the in-plane shear stress; this observation is valid even when transverse shear deformation effects are considered.

To compare the numerical results with the analytical values predicted using Eq. (18),  $\varepsilon_{xy}$  at the center point (0, 0, 5.1 mm) are plotted in Fig. 2 as a function of increasing load.

The analytical and numerical values are in close agreement, and their differences increase with increasing load. Overall, Eq. (18) provides good accuracy in predicting  $\varepsilon_{xy}$ . For a load of 450 N, the maximum difference between the analytical and numerical values at the plate center is 4%. Because the analytical derivation of  $\varepsilon_{xy}$  with the transverse shear deformation effects included has the identical form as the classical analysis, this comparison indicates that, for the material and lay-up configuration evaluated, the transverse shear deformation effects can be neglected in determining the in-plane shear modulus or strength of the laminated composite plate structures without losing accuracy.

#### IV. Experimental Validation

Laminated composite plates were fabricated at the Center for Composite Materials at the University of Delaware for testing. The

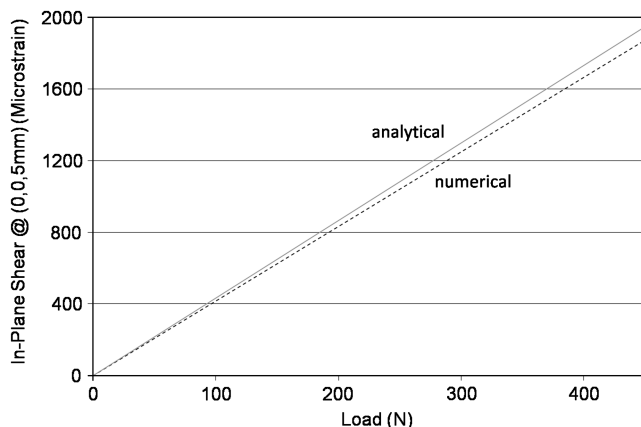


Fig. 2 Comparison of the analytical and numerical values for  $\varepsilon_{xy}$  at the center point of the laminate plate.

laminate is cross-ply with top and bottom face layers having the same direction as the global coordinate. The prototype plate consists of 22 equal-thickness layers stacked symmetrically about the midplane. The fiber and matrix materials are plain E-glass and epoxy vinyl ester resin, respectively. The laminate has overall dimensions of  $431.8 \times 431.8 \times 13$  mm, and a fiber volume fraction of 55%.

According to the properties provided by the manufacturer,  $G_{12f} = 28.57$  GPa,  $\nu_{12f} = 0.26$ , and  $G_m = 1.38$  GPa. Hence, for this laminated plate, the in-plane shear modulus  $G_{12}$  can be computed using [6]:

$$G_{12} = G_m \frac{1 + \eta V_f}{1 - \eta V_f}$$

where

$$\eta = \frac{G_{12f}/G_m - 1}{G_{12f}/G_m + 1}$$

It is seen that  $\eta = 0.91$  and  $G_{12} = 4.14$  GPa. Furthermore,  $D_{66}$  of the plate is computed as  $706.16$  N · m. Using Eq. (18), the face strains of the laminate at any load can be predicted.

The laminate was mounted in an Instron testing machine using the mounting fixture and configuration shown in Fig. 3. The face strains were measured at seven strain gage locations shown in Fig. 4.

Strain gages 1 and 7 are placed along the  $x$  and  $y$  directions to measure the normal strains. Gages 2–6 are placed diagonally to measure the in-plane shear strains assuming  $|\varepsilon_{\text{diagonal}}| = |\varepsilon_{xy}|$  according to the strain transformation (assuming no normal strains). During each experiment, to avoid nonlinear deformation effects, load magnitudes were limited such that the lateral deflections at the corners of the plate were less than half the plate thickness.

The experimental data show that the in-plane normal strains are almost zero compared with the in-plane shear strain,  $\varepsilon_{xy}$ . All the linear analyses with or without the transverse shear deformation effects have predicted that there are no in-plane normal strains (i.e.,  $|\varepsilon_{\text{diagonal}}| = |\varepsilon_{xy}|$ ). Both the finite element results and the experimental data confirm this relationship.

As an additional check, the experimentally measured strain at gauge location 3 in Fig. 4 was used to estimate the actual properties of the plate using Eq. (18). Estimates of  $D_{66}$  and  $G_{12}$  were  $847$  N · m and  $4.63$  GPa, respectively. This translates to about an 11% difference for  $G_{12}$  compared to the  $4.14$  GPa value computed based on the micromechanics relation.

It was observed throughout the experimental data that the tensile strain values measured at point 2 were somewhat smaller than the tensile strain values measured at points 3 and 4. It is possible that the strain gage placed at point 2 was not mounted exactly along the diagonal direction, which is the principle direction.

Figure 5 contains the measured strain values at points 3–6 as a function of increasing load. To compare the magnitudes of  $\varepsilon_{xy}$  at these points, all data are plotted as absolute values. It is seen that the in-plane shear strains at different points fall into a relatively narrow range. As predicted from Eq. (18), the in-plane shear strains have the same magnitude everywhere on the plate surface, and the experimental data confirm this behavior. The small difference between the values at different points can be explained by experimental errors such as the mounting direction of the gages. It also can be seen in Fig. 4 that the magnitudes of the shear strains at points 5 and 6, which are compressive strains, are larger than those at points 3 and 4, which are tensile strains. This difference can be explained by the unique material properties in tension versus compression. This same conclusion has been proposed by ASTM [8].

Figure 6 compares the analytical values with the strain data measured at point 6, which have the maximum absolute values, and those at point 3, which have the minimum absolute values.

All experimental data are less than the analytical results by 17–29%. This difference can be attributed to several factors including the actual loading condition in the experiments, misalignment of the

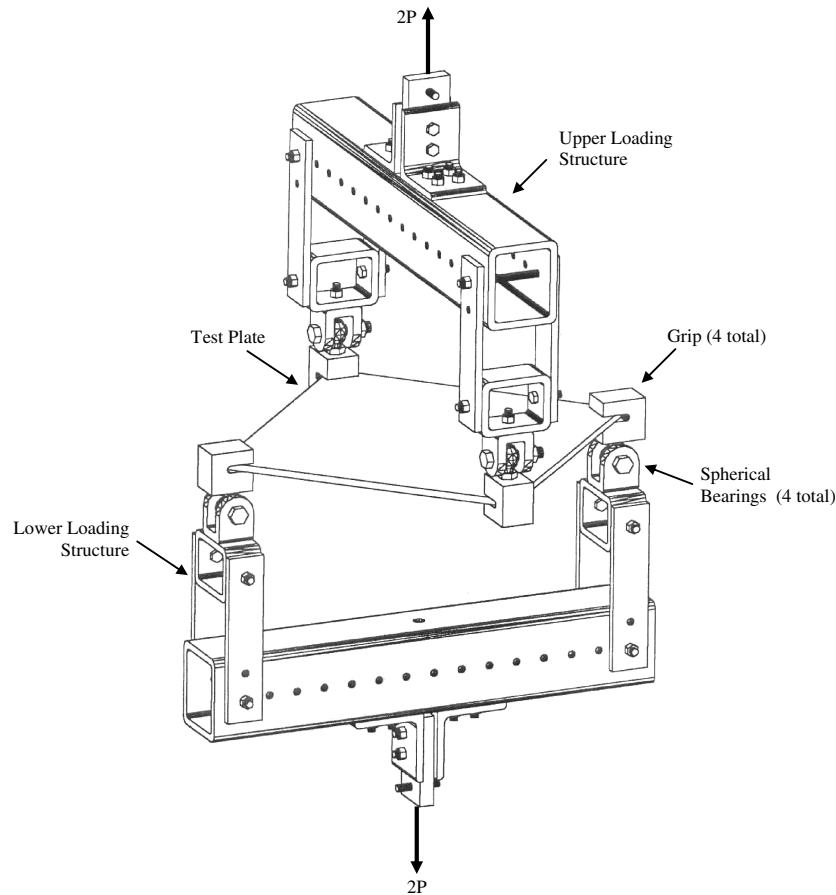


Fig. 3 Schematic of the test fixture used to create the plate loading illustrated in Fig. 1.

loading points in the test fixture, and slippage in the grips. Regarding the load condition that occurred in the experiments, the grips illustrated in Fig. 3 contact the plate and apply the loads over small areas at each of the plate corners. This loading configuration is different than the idealized situation used in the analytical model where point loads were assumed to be applied at the corners of the plate.

To understand the effects of the actual loading condition on the predicted strains, the finite element models were modified to better reflect the actual loading by the grips. To accomplish this, loads were assumed to be uniformly distributed under the grip face in contact with the plate ( $10 \text{ cm}^2$ ). Simulations with this more accurate loading representation revealed a decrease in strain magnitudes compared with the ideal point-loading condition. This computational result confirms the above explanation [9].

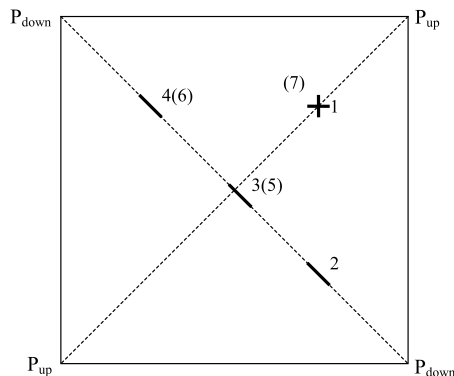


Fig. 4 Strain gage locations and numbering system used during testing of the prototype laminate plate. Numbers in brackets indicate gage locations on the reverse side of the plate.

Numerical and experimental studies were also carried out on foam core sandwich plates. However, due to the extremely low flexural stiffness of the plates, large deflections occurred under small loads (less than 44 N). The plates exhibit obvious nonlinear behavior, a similar phenomenon observed in the previous study conducted by Ebrahimpour et al. [3]. As a result, the linear analysis developed in this study is not suitable for that case. Additional analysis considering the geometrically nonlinear deformation effects has been developed to explain the behavior of the foam core sandwich plates [4]. However, for the sandwich plates having relatively high flexural stiffness, that is, when the nonlinear deformation effects can be ignored, the analysis developed herein, verified by the computation and testing of the laminate plates, can be applied to describe their behavior.

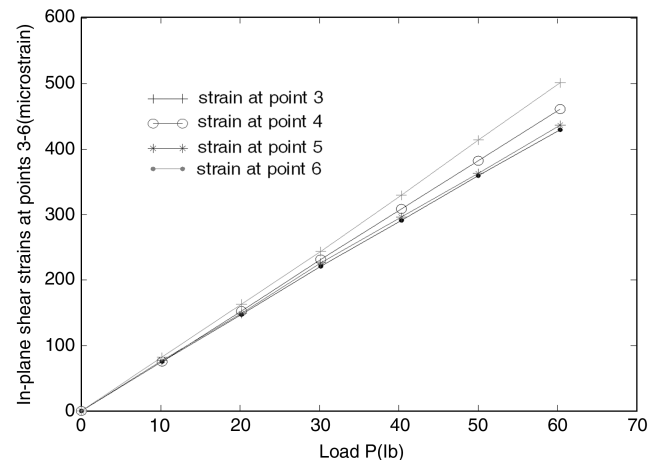


Fig. 5 Comparison of the measured diagonal strains at different points on the laminated plate.

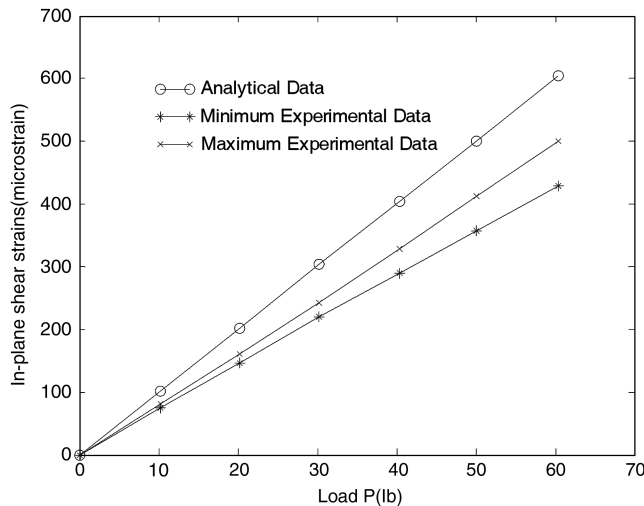


Fig. 6 Comparison of the analytical and experimental values of  $|\epsilon_{xy}|$  for the laminated plate.

## V. Conclusions

Based upon the analytical results and comparisons with the numerical and experimental results, some conclusions can be summarized for the in-plane shear test as follows:

- 1) The analysis including the transverse shear deformation effects indicates that these effects do not influence the in-plane shear strains and stresses, when compared with the classical plate theory analysis. However, they do affect the lateral deflection and is reflected by an additional term  $3[(A_{55}b^2 + A_{44}a^2)/A_{44}A_{55}a^2b^2]P_{xy}$  in the lateral displacement function. The transverse shear deformation effects decrease with increasing cross-thickness transverse shear moduli. When  $A_{44}$  and  $A_{55}$  approach infinity, the results revert to the same form as derived by classical plate theory.
- 2) Both the numerical and experimental results verify the linear analytical results in that the normal in-plane strains are sufficiently small that they can be neglected.
- 3) The in-plane shear strain is independent of the in-plane positions  $x$  and  $y$ . At a given depth  $z$ , this strain is uniform everywhere in the plate.
- 4) The transverse shear strains are much smaller than the in-plane shear strain for laminate plates.
- 5) Within the linear deformation range, the transverse shear deformation effects can be ignored for the laminate composite plates studied. According to the analysis, the transverse shear deformation effects will be significant only for plates having very low ratios of the transverse shear moduli to the in-plane shear modulus.
- 6) Both the analytical and numerical results verify the linear relation between the in-plane shear strain and the applied vertical load. Although the numerical data agree with the analytical data, the experimental data are smaller in magnitude than the analytical values due to the geometry of the fixtures used in the experiments.

7) Nonlinear behavior is found in foam core sandwich plates with low flexural stiffness. Numerical and experimental studies of other types of sandwich plates are necessary to verify the analytical results. For sandwich plates having relatively high flexural stiffness, the analytical results developed in this study, which are verified with laminate plates, are expected to be valid.

8) Within a small deflection range, the analytical expression

$$[\epsilon_{xy}]_k = -\frac{P}{4D_{66}}z$$

is a very accurate approximation for composite plates subjected to the in-plane shear loads. Using this relationship along with the strain-stress relations and constitutive equations of the composite plates, the in-plane shear modulus and the in-plane shear strength can be accurately determined.

9) In sandwich plate structures, because the in-plane shear stresses are linear in the thickness direction, one can design the plate construction to force failure either in the faces or in the core. Therefore, the intended strength can be determined.

10) Because the in-plane shear stresses are constant in the coordinates  $x$  and  $y$ , this test may be used as a quality control means, by subjecting the plate to a percentage of the failure load to insure proper manufacturing, etc.

## References

- [1] Nadai, A., *Die Elastischen Platten*, Springer-Verlag, Berlin, 1925.
- [2] Vinson, J. R., "In-Plane Shear Strength Determination of Composite Materials in Laminated and Sandwich Panels," *Proceedings of Applied Mechanics Reviews, ASME*, Vol. 50, No. 11, Pt. 2, 1997, pp. 5237-5240.
- [3] Ebrahimpour, A., Vinson, J. R., and Thomsen, O. T., "Experimental and Analytical Study on the Behavior of Foam Core Sandwich Composite Plates Subjected to In-plane Shear Stress," AIAA Paper 2001-1220, 2001.
- [4] Wang, J., Vinson, J. R., and Glancey, J. L., "Geometric Nonlinear Deformation Effects in Composite Sandwich Plates Subject to In-Plane Shear Loads," *Journal of Sandwich Structures and Materials*, Vol. 6, No. 5, 2004, pp. 447-457.  
doi:10.1177/1099636204040334
- [5] Kant, T., and Swaminathan, K., "Analytical Solution for the Static Analysis of Laminated Composite and Sandwich Plates Based on a Higher Order Refined Theory," *Composite Structures*, Vol. 56, No. 4, 2002, pp. 329-344.  
doi:10.1016/S0263-8223(02)00017-X
- [6] Vinson, J. R., and Sierakowski, R. L., *The Behavior of Structures Composed of Composite Materials*, 2nd ed., Kluwer Academic Publishers, The Netherlands, 2002.
- [7] ANSYS, *ANSYS Theory Reference*, ANSYS, Canonsbury, PA, 2000.
- [8] *Standard Guide for Testing In-plane Shear Properties of Composites Laminates*, Annual Book of ASTM Standards, ASTM, West Conchohocken, PA, 1989, Vol. 15.03, D4255-83.
- [9] Wang, J., "Behavior of Isotropic and Composite Plates Subjected to In-plane Shear Loads," M.S. Thesis, Department of Mechanical Engineering, University of Delaware, 2002.